

Bowing Effect on Elastic Stability for Members Having Concave Configuration Shapes

Dr. Wisam Victor Yossif

***Water Resources Engineering Department, College of Engineering
Baghdad University, Baghdad, Iraq***

Abstract

The Non-linear analysis of members having concave configuration shapes is considered using stability functions. The accuracy of results has been verified by using the finite element method by discretizing the beam-column member into different numbers of an equivalent prismatic element.

The change of member lateral stiffness and change of member length are considered by using the stability and bowing functions after deriving them here.

The axial deformation of concave beam-column including the effect of bowing is compared with the same of that without bowing effect to estimate the exact deformation of the beam-column under the same boundary condition and applied load.

الخلاصة

تمت دراسة التحليل اللاخطي للعتبات ذات الأشكال المقعرة باستخدام دوال الاستقرار. ومن ثم دقت النتائج باستخدام طريقة العناصر المحددة بواسطة تقسيم العتبة الى عتبات موشورية مكافئة.

تمت دراسة تغيير قيمة الصلابة للعتبة و تغيير طول العتبة من خلال استخدام دوال الاستقرار والتحدب بعد اشتقاقها.

تمت مقارنة التشوه المحوري للعتبات المقعرة المتضمن تأثير التحدب مع نفس العتبات الغير المتضمن تأثير التحدب لتقييم التشوهات الدقيقة للعتبات تحت نفس الظروف ونفس الأحمال.

1. Introduction

The nonlinear effect is considered for slender beam-column members loaded axially. The member bends and deflects laterally under the increase of axial load until buckling occurs, the member stiffness is considered as a function of axial load which is expressed mathematically by deriving the stability functions.

The effect of flexural bending on axial stiffness and the effect of axial force on the flexural stiffness produce an additional stiffness expressed mathematically by the bowing functions.

In most previous studies, the research developments had dealt with prismatic beam-column members and little attention had been paid to buckling load of non-prismatic members. The effect of pre-buckling deformations in the stability analysis of members had been ignored by most researchers for simplicity, however Mansur et. al. and Hayashi (as cited in reference 2) studied the effect of axial strain due to flexural deformations. Oran^[3, 4] obtained the tangent stiffness matrix and studied the geometric nonlinearity of non-prismatic members of linearly varying depth. Goto et. al.^[2] derived the closed form tangent stiffness equation from the consistent beam-column theory considering the change in length of the member axis.

The finite element method has been used for geometric nonlinear analysis and for the evaluation of buckling loads for prismatic beam-column members.

2. Derivation of Stability Functions

The equations of slope-deflection for a prismatic member in terms of the stability functions s and sc are given below^[7]:

$$M_1 = \frac{EI_2}{L} (s\theta_1 + sc\theta_2) \dots\dots\dots (1)$$

$$M_2 = \frac{EI_2}{L} (sc\theta_1 + s\theta_2) \dots\dots\dots (2)$$

Also the other two equations of slope-deflection for a non-prismatic member in terms of the stability functions S_1 , S_2 and SC are given below:

$$M_1 = \frac{EI_1}{L} (S_1\theta_1 + SC\theta_2) \dots\dots\dots (3)$$

$$M_2 = \frac{EI_1}{L} (SC\theta_1 + S_2\theta_2) \dots\dots\dots (4)$$

where:

$M_1, M_2, \theta_1, \theta_2$ and L : are as defined in Fig.(1).

The derivation of the stability functions by the exact method is presented here for a third degree of nonlinear concave tapered members as shown in **Fig.(1)** and having a rectangular cross section bent about major axis.

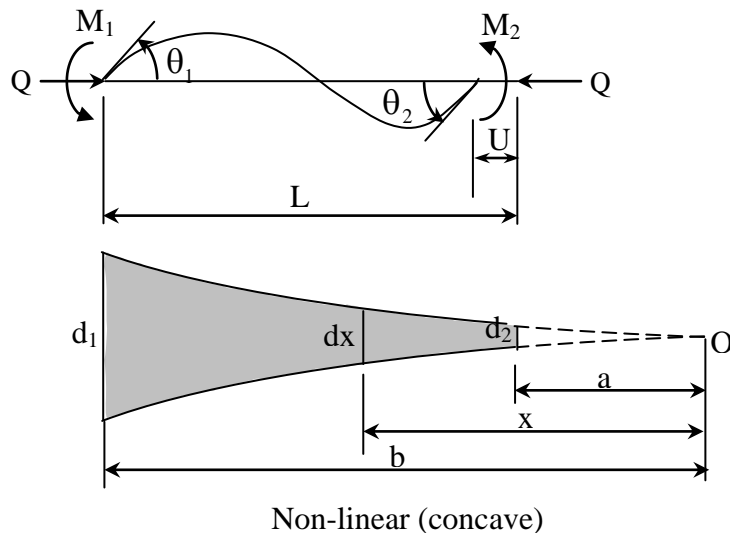


Figure (1) A third degree tapered beam-column element

The depth $d(x)$ may be expressed by:

$$d(x) = d_2(x/a)^3 \dots\dots\dots (5)$$

where:

$d(x)$: is the non-linear depth.

From Equation (5), the depth at end 1 can be obtained as:

$$d_1 = d_2(b/a)^3 \dots\dots\dots (6)$$

The moment of inertia $I(x)$ of the strut at distance x from the origin O may be expressed as:

$$I(x) = \frac{b_o[d(x)]^3}{12} \dots\dots\dots (7)$$

By substituting Equation (5) into Equation (7), the moment of inertia $I(x)$ is:

$$I(x) = I_2(x/a)^9$$

where:

$$I_2 = \frac{b_o d_2^3}{12} \dots\dots\dots (8)$$

The basic differential equation of the concave beam-column subjected to constant axial force Q and end moments M₁ and M₂ is ^[1]:

$$EI(x) \frac{d^2y}{dx^2} + Qy = \frac{M_1}{L}(x-a) + \frac{M_2}{L}(x-b) \dots\dots\dots (9)$$

Substituting Equation (7) into Equation (9) yields:

$$EI_2 \left(\frac{x}{a}\right)^9 \frac{d^2y}{dx^2} + Qy = \frac{M_1}{L}(x-a) + \frac{M_2}{L}(x-b) \dots\dots\dots (10)$$

The right hand side of Equation (10) can be reduced to zero by substituting the term “z” as follows:

$$z = y - \frac{M_1}{QL}(x-a) - \frac{M_2}{QL}(x-b) \dots\dots\dots (11)$$

Thus, the differential equation becomes:

$$\frac{d^2z}{dx^2} + \frac{\omega^2 z}{x^9} = 0 \dots\dots\dots (12)$$

where:

- E*: Modulus of Elasticity
- I₂*: The moment of inertia at end 2 of the member
- I(x)*: The moment of inertia at distance *x* from the origin *O*
- M₁, M₂*: Bending moments at member ends 1 and 2 respectively
- S₁, SC, S₂*: The stability functions of concave taper members
- Q*: Axial force
- a*: The distance of end 2 from the origin *O*
- b*: The distance of end 1 from the origin *O*
- b_o*: Constant member width
- d₁, d₂*: The depths at ends 1 and 2 as shown in **Fig.(1)**
- y*: Lateral deflection of member
- ω^2 : Qa^9/EI_2

Equation (10) can be transformed into Bessel Equation of the following form ^[5,6]:

$$\frac{d^2z}{dx^2} - \frac{(2\bar{\alpha}-1)}{x} \cdot \frac{dz}{dx} + \left(\bar{\beta}^2 \gamma^2 x^{2\gamma-2} + \frac{\bar{\alpha}^2 - n^2 \gamma^2}{x^2} \right) z = 0 \dots\dots\dots (13)$$

By equating Equations (12) and (13), the constants $\bar{\alpha}, \bar{\beta}, \gamma$ and *n* can be obtained:

$$\bar{\alpha} = 0.5, \quad \bar{\beta} = \left| \frac{2\omega}{2-9} \right| = 0.287\omega, \quad \gamma = \frac{2-9}{2} = -3.5, \quad n = \pm \frac{1}{2-9} = \pm 0.143$$

This equation has a general solution of [5]:

$$z = x^{\bar{\alpha}} \left[A J_n(\bar{\beta} x^\gamma) + B J_{-n}(\bar{\beta} x^\gamma) \right] \dots\dots\dots (14)$$

J_n is the Bessel function of order n for $\bar{\beta} x^\gamma$:

$$J_n(\bar{\beta} x^\gamma) = \sum_{r=0}^{\infty} (-1)^r \frac{(0.5 \bar{\beta} x^\gamma)^{n+2r}}{r!(n+r)!} \dots\dots\dots (15)$$

The solution of Equation (10) can be written down in terms of Bessel functions and the constants $\bar{\alpha}, \bar{\beta}, \gamma$ and n .

$$y = x^{0.5} \left[A J_{0.143} \left(\frac{0.286\omega}{x^{3.5}} \right) + B J_{-0.143} \left(\frac{0.286\omega}{x^{3.5}} \right) \right] + \frac{M_1}{QL} (x-a) + \frac{M_2}{QL} (x-b) \dots\dots\dots (16)$$

The constants A, and B are obtained from the following boundary conditions:

at $x = a$, $y = 0$ and $dy/dx = \theta_2$.

and $x = b$, $y = 0$ and $dy/dx = \theta_1$.

$$A = \frac{M_1 J_{-0.143}(\alpha) \sqrt{a} + M_2 J_{-0.143}(\beta) \sqrt{b}}{\sqrt{a} \sqrt{b} ZQ} \dots\dots\dots (17)$$

$$B = - \frac{M_1 J_{0.143}(\alpha) \sqrt{a} + M_2 J_{0.143}(\beta) \sqrt{b}}{\sqrt{a} \sqrt{b} ZQ} \dots\dots\dots (18)$$

where:

$$Z = J_{0.143}(\alpha) J_{-0.143}(\beta) - J_{-0.143}(\alpha) J_{0.143}(\beta) \dots\dots\dots (19)$$

$$\alpha = 0.286 \frac{\omega}{a^{3.5}} \quad , \quad \beta = 0.286 \frac{\omega}{b^{3.5}}$$

After that the end rotations θ_1 and θ_2 can be obtained from the first derivative of Equation (16). In view of Equation (3) and (4), the stability functions [6,7] S_1, S_2 and SC are:

$$S_1 = \left(\omega L f_4 + Z a^{4.5} \right) \left(\frac{-LZQ b^{4.5}}{\omega P E I_2} \right) \dots\dots\dots (20)$$

$$SC = \left(\omega L f_5 + Z a^{0.5} b^4 \right) \left(\frac{LZQ a^4 b^{0.5}}{\omega P E I_2} \right) \dots\dots\dots (21)$$

$$S_2 = (\omega L f_3 + Z b^{4.5}) \left(\frac{-LZQa^{4.5}}{\omega P E I_2} \right) \dots\dots\dots (22)$$

where:

$$P = Z \left[a^4 \left(\frac{f_5}{b^{-0.5}} - \frac{f_3}{a^{-0.5}} \right) - b^4 \left(\frac{f_4}{b^{-0.5}} - \frac{f_6}{a^{-0.5}} \right) \right] - \omega L f_1 f_2 \dots\dots\dots (23)$$

where:

f₁, f₂, f₃, f₄, f₅ and f₆: are given in Appendix A.

3. Bowing Effect

The total axial deformation of the beam-column is defined by U, which is the summation of the axial deformation due to the axial force U_a and flexural deformation U_b due to bending:

$$U = U_a + U_b \dots\dots\dots (24)$$

$$U_a = \frac{QL}{EA_o} \dots\dots\dots (25)$$

$$U_b = C_b L = L_d - L \dots\dots\dots (26)$$

where:

Q: The axial force

L_d: Deflected length of beam-column member

L : Length of beam-column

C_b: Length correction factor due to bowing

A_o: Equivalent cross-section area of beam-column^[4], $A_o = A_2 \left[\frac{(d_1/d_2)-1}{\ln(d_1/d_2)} \right]$ ^[11]

A₂: Cross-section area at smaller depth at end 2.

For prismatic members^[4]:

$$C_b = b_1(\theta_1 + \theta_2)^2 + b_2(\theta_1 - \theta_2)^2 \dots\dots\dots (27)$$

where:

$$b_1 = -\frac{C'_1 + C'_2}{4\pi^2} \dots\dots\dots (28)$$

$$b_2 = -\frac{C'_1 - C'_2}{4\pi^2} \dots\dots\dots (29)$$

where:

$$C'_1 = s' = \frac{\partial s}{\partial \rho} \quad \text{and} \quad C'_2 = sc' = \frac{\partial sc}{\partial \rho}$$

ρ : is the non-dimensional axial force parameter for prismatic member

The bowing function and length correction factor of linearly tapered non-prismatic members derived by Oran, which are used to derive the same functions for concave non-prismatic members are as below [1,4]:

$$\bar{C}_b = \beta_1 \theta_1^2 + 2\beta_2 \theta_1 \theta_2 + \beta_3 \theta_2^2 \dots\dots\dots (30)$$

$$\beta_1 = -\frac{S'_2}{2\pi^2} \dots\dots\dots (31)$$

$$\beta_2 = -\frac{SC'}{2\pi^2} \dots\dots\dots (32)$$

$$\beta_3 = -\frac{S'_1}{2\pi^2} \dots\dots\dots (33)$$

$$S'_1 = \left[h_1 - h_4 + \frac{Z'}{\omega} \right] \frac{Z\omega\rho\pi^2}{PL} (ab)^{4.5} \dots\dots\dots (34)$$

$$SC' = \left[-h_3 + h_6 + \frac{Z'}{\omega} \right] \frac{Z\omega\rho\pi^2}{PL} (ab)^{4.5} \dots\dots\dots (35)$$

$$S'_2 = \left[h_2 - h_5 - \frac{Z'}{\omega} \right] \frac{Z\omega\rho\pi^2}{PL} (ab)^{4.5} \dots\dots\dots (36)$$

where:

b_1, b_2 : Bowing function of prismatic member

$\beta_1, \beta_2, \beta_3$: Bowing function of non-prismatic member

S'_2, SC', S'_1 : First derivative of stability function of non-prismatic member

where:

h_1, h_2, h_3, h_4, h_5 and h_6 are as defined in **Appendix A**.

4. Tangent Stiffness Matrix

The tangent stiffness matrix is the relation between incremental forces and end deformations in which the end forces can be expressed from the modified slope-deflection equations as given in Equations (3), (4) and the relation between axial force and bowing effect is given in Equation (37):

$$QL = EA_o L \left(\frac{\rho \pi^2}{\lambda^2} + \bar{C}_b \right) \dots\dots\dots (37)$$

The relations between incremental values of end forces ΔF and end deformations Δu can be expressed in matrix form as:

$$\{\Delta F\} = [T]\{\Delta u\} \dots\dots\dots (38)$$

in which [T] is the tangent stiffness matrix for relative deformations ^[1] which are derived in Equations (39) for non-prismatic member:

$$T_{ij} = \frac{\partial F_i}{\partial u_j} + \frac{\partial F_i}{\partial \rho_2} \cdot \frac{\partial \rho_2}{\partial u_j} \dots\dots\dots (39)$$

This is equal to:

$$[T] = \begin{bmatrix} \frac{\partial M_1}{\partial \theta_1} + \frac{\partial M_1}{\partial \rho_2} \frac{\partial \rho_2}{\partial \theta_1} & \frac{\partial M_2}{\partial \theta_1} + \frac{\partial M_2}{\partial \rho_2} \frac{\partial \rho_2}{\partial \theta_1} & \frac{\partial(QL)}{\partial \theta_1} + \frac{\partial(QL)}{\partial \rho_2} \frac{\partial \rho_2}{\partial \theta_1} \\ \frac{\partial M_1}{\partial \theta_2} + \frac{\partial M_1}{\partial \rho_2} \frac{\partial \rho_2}{\partial \theta_2} & \frac{\partial M_2}{\partial \theta_2} + \frac{\partial M_2}{\partial \rho_2} \frac{\partial \rho_2}{\partial \theta_2} & \frac{\partial(QL)}{\partial \theta_2} + \frac{\partial(QL)}{\partial \rho_2} \frac{\partial \rho_2}{\partial \theta_2} \\ \frac{\partial M_1}{\partial(U/L)} + \frac{\partial M_1}{\partial \rho_2} \frac{\partial \rho_2}{\partial(U/L)} & \frac{\partial M_2}{\partial(U/L)} + \frac{\partial M_2}{\partial \rho_2} \frac{\partial \rho_2}{\partial(U/L)} & \frac{\partial(QL)}{\partial(U/L)} + \frac{\partial(QL)}{\partial \rho_2} \frac{\partial \rho_2}{\partial(U/L)} \end{bmatrix} \dots (40)$$

By substituting the equations given in appendix B into Equation (40), the tangent stiffness matrix including bowing effect can be derived in the form below ^[8]:

$$[T] = \frac{EI_2}{L} \begin{bmatrix} \frac{S_1}{u^m} + \frac{G_1^2}{\pi^2 H} & \frac{SC}{u^m} + \frac{G_1 G_2}{\pi^2 H} & \frac{G_1}{H} \\ \frac{SC}{u^m} + \frac{G_1 G_2}{\pi^2 H} & \frac{S_2}{u^m} + \frac{G_2^2}{\pi^2 H} & \frac{G_2}{H} \\ \frac{G_1}{H} & \frac{G_2}{H} & \frac{\pi^2}{H} \end{bmatrix} \dots\dots\dots (41)$$

where:

$$\lambda = \frac{L}{\sqrt{I_2 / A_o}}$$

u: Taper ratio, $=b/a=(d_1/d_2)^{1/3}$

m: Shape factor, $\log(I_1 / I_2) / \log u$ reference (8, 9), in this study ($m=9$)

$$G_1 = -2\pi^2 [\beta_1 \theta_1 + \beta_2 \theta_2], G_2 = -2\pi^2 [\beta_2 \theta_2 + \beta_3 \theta_1], H = \frac{\pi^2}{\lambda^2} + \beta_1' \theta_1^2 + 2\beta_2' \theta_1 \theta_2 + \beta_3' \theta_2^2$$

and,

$$\beta'_1 = -\frac{S''_2 u^m}{2\pi^2} \dots\dots\dots (42)$$

$$\beta'_2 = -\frac{SC'' u^m}{2\pi^2} \dots\dots\dots (43)$$

$$\beta'_3 = -\frac{S''_1 u^m}{2\pi^2} \dots\dots\dots (44)$$

in which,

$$S''_1 = (g_1 + g_4) \frac{Z\omega\rho\pi^2(ab)^{4.5}}{PL} \dots\dots\dots (45)$$

$$SC'' = (g_3 + g_6) \frac{Z\omega\rho\pi^2(ab)^{4.5}}{PL} \dots\dots\dots (46)$$

$$S''_2 = (g_2 + g_5) \frac{Z\omega\rho\pi^2(ab)^{4.5}}{PL} \dots\dots\dots (47)$$

Appendix A defines the symbols g_1, g_2, g_3, g_4, g_5 and g_6 .

where:

$\beta'_1, \beta'_2, \beta'_3$: First derivative of bowing functions

S''_2, SC'', S''_1 : Second derivative of stability functions of non-prismatic member

u^m : Tapering ratio to the power of shape factor

The stability and bowing values with respect to non-dimensional axial force parameter for five different cases of tapering ratio $u = 1.5, 2.0, 3.0, 4.0$ and 5.0 for constant member length are presented graphically in **Figs.(2), (3), (4), (5)** and **(6)** for beam-column subjected to compressive axial force starting from zero.

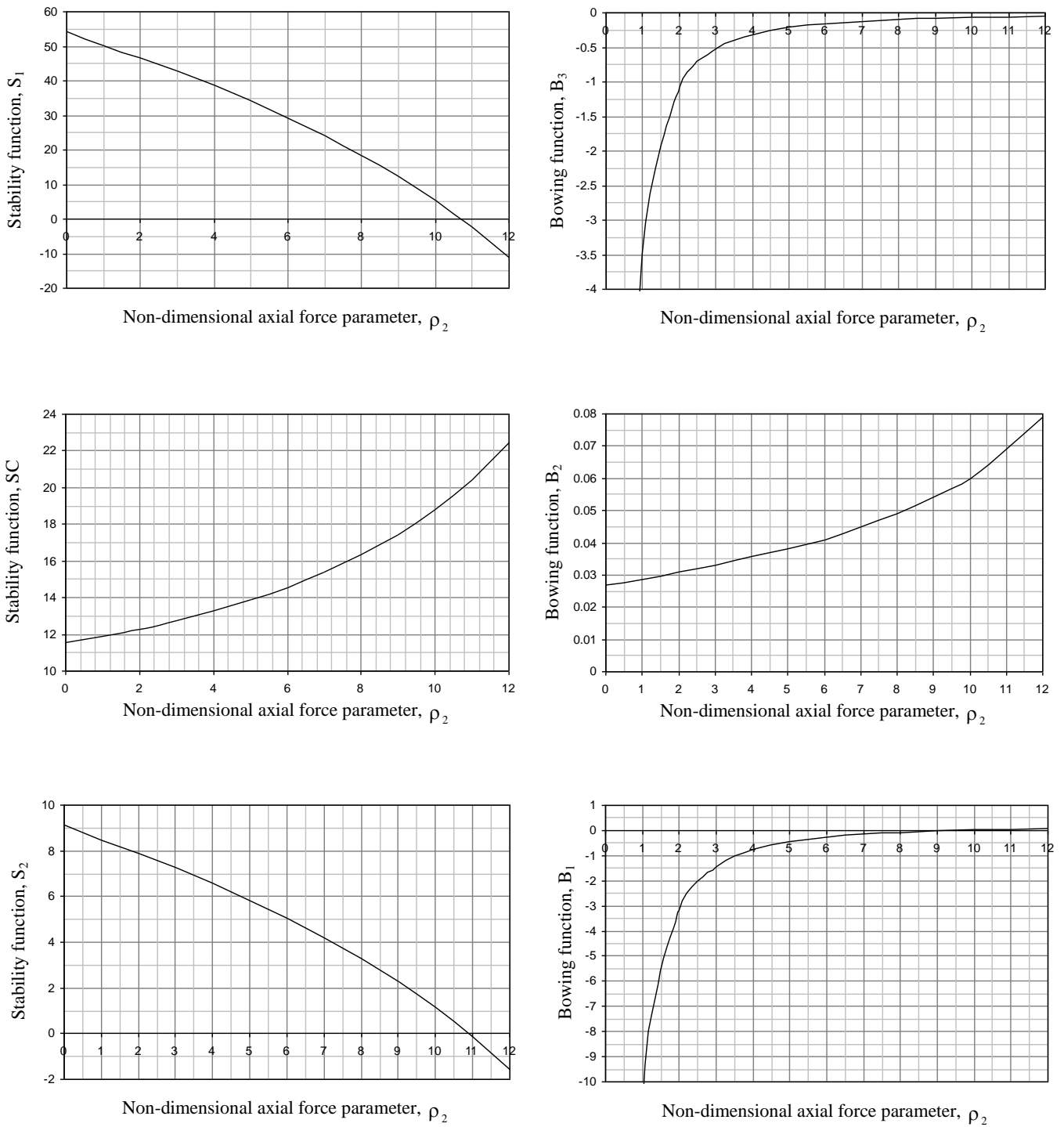


Figure (2) Stability and bowing functions for concave configuration beam-column in tapering ratio $u = 1.5$

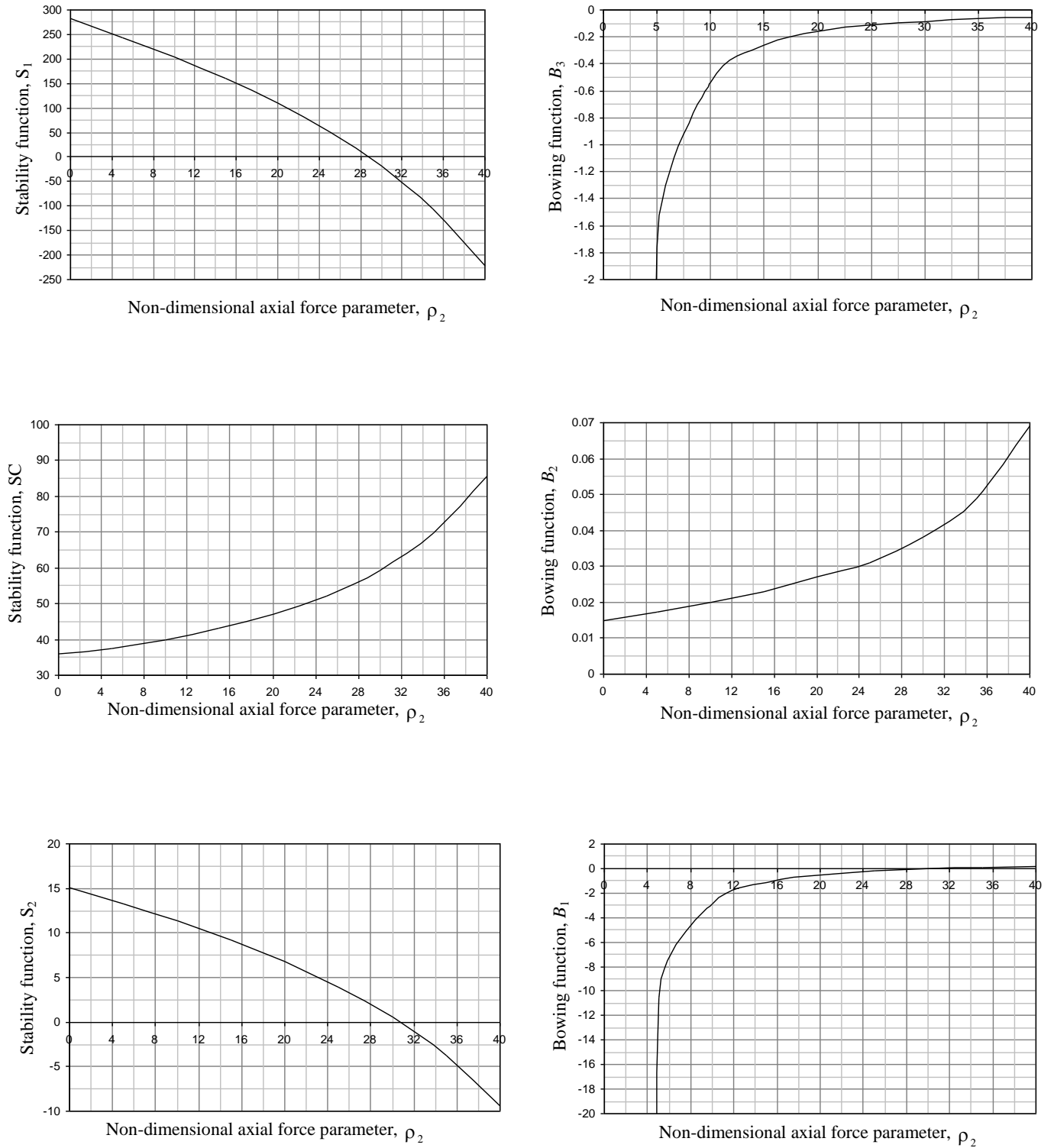


Figure (3) Stability and bowing functions for concave configuration beam-column in tapering ratio $u = 2.0$

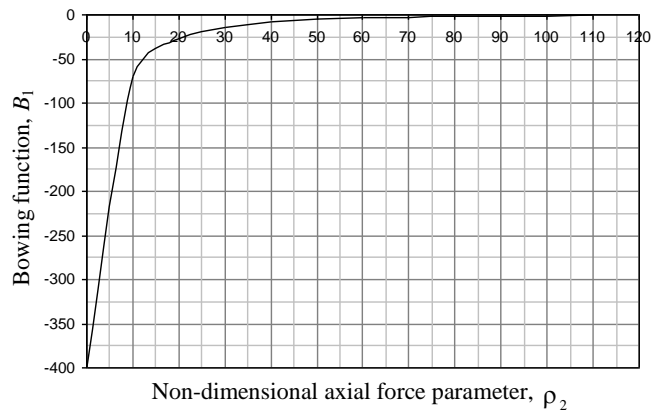
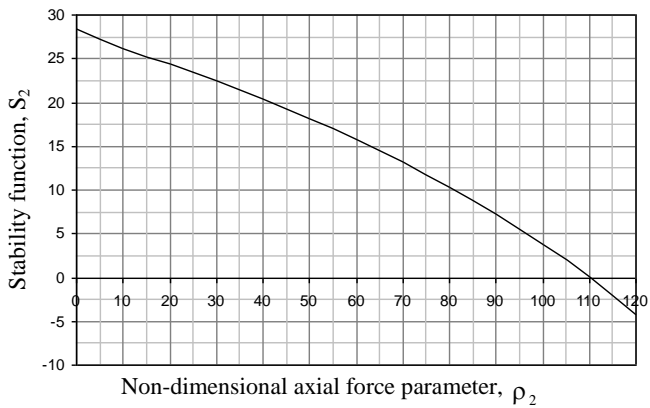
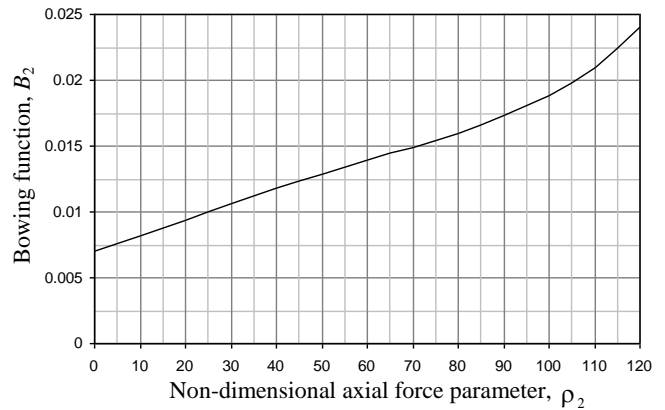
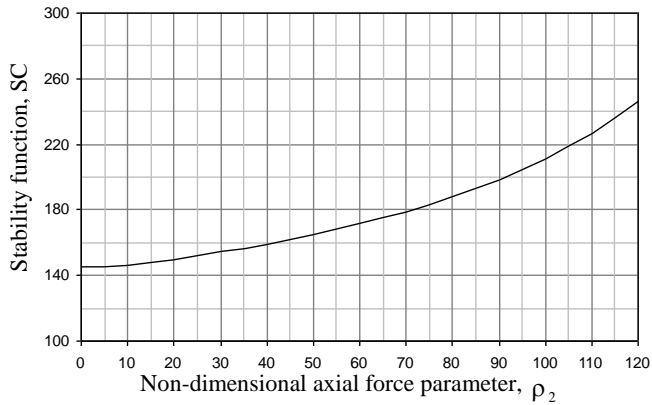
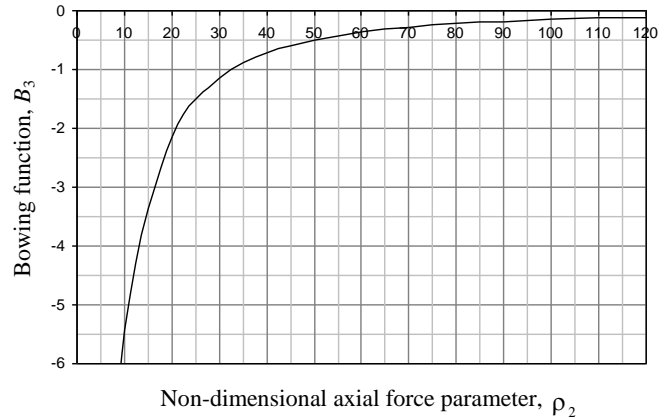
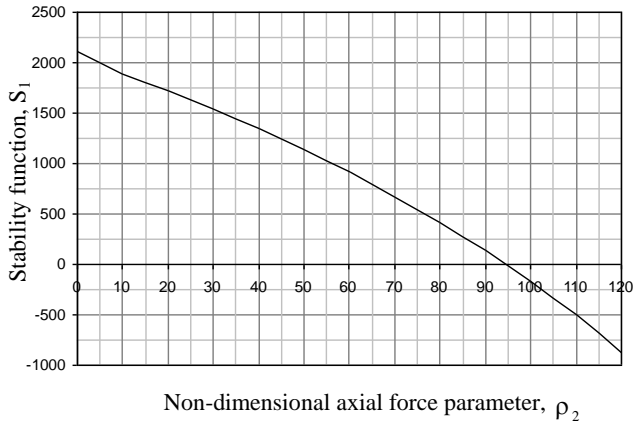


Figure (4) Stability and bowing functions for concave configuration beam-column in tapering ratio $u = 3.0$

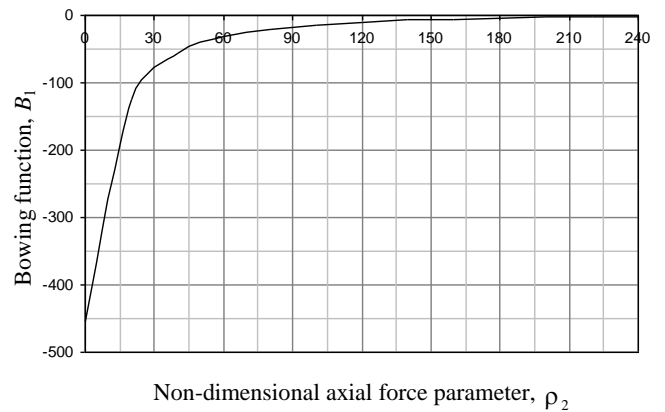
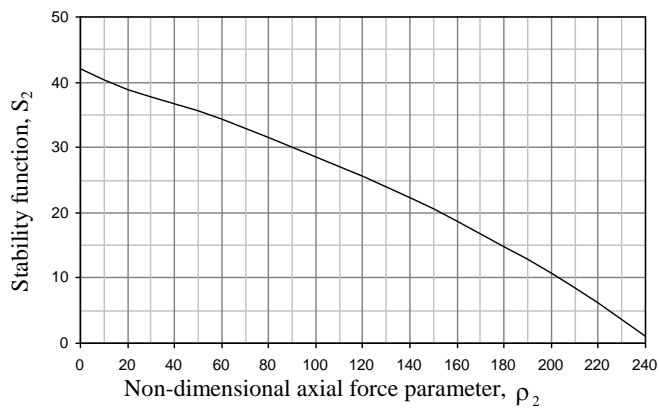
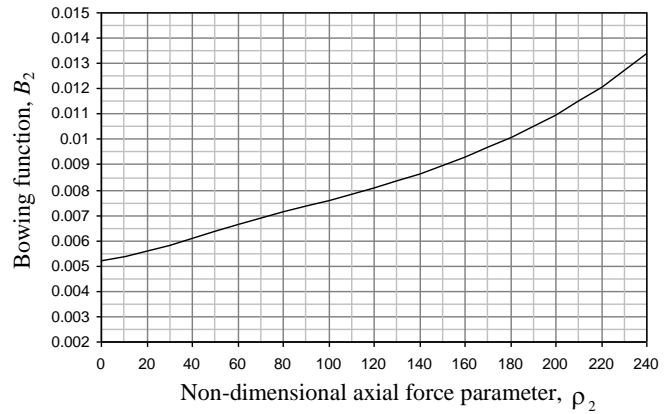
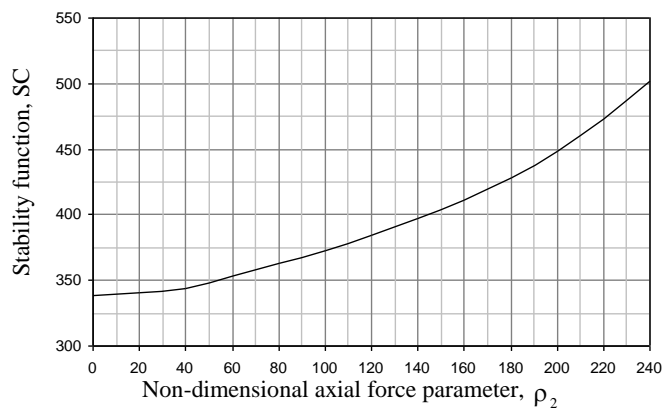
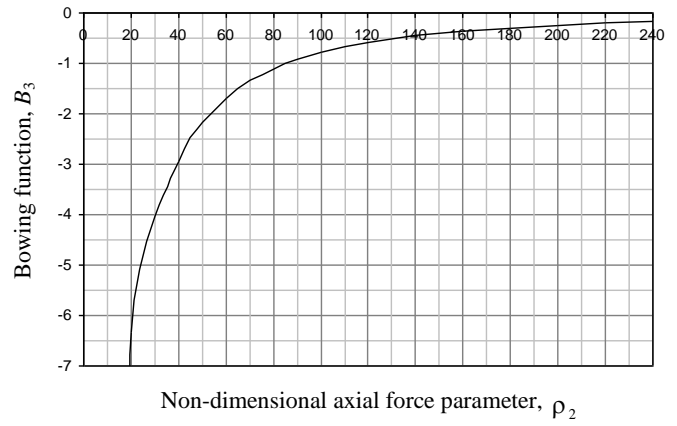
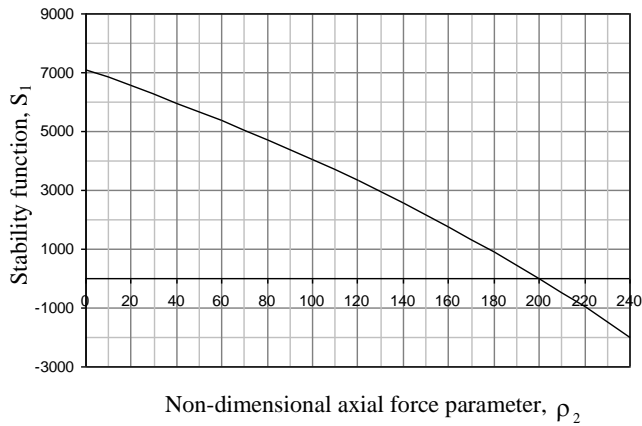
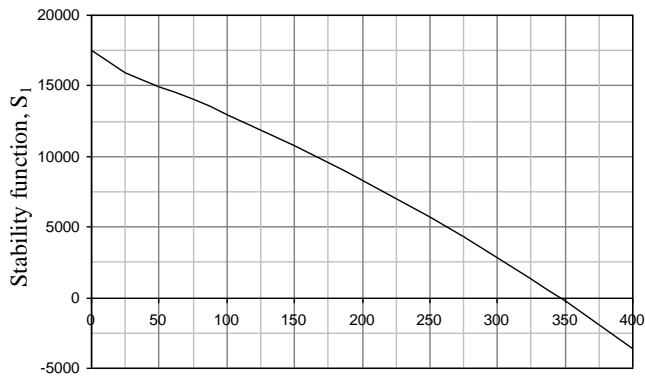
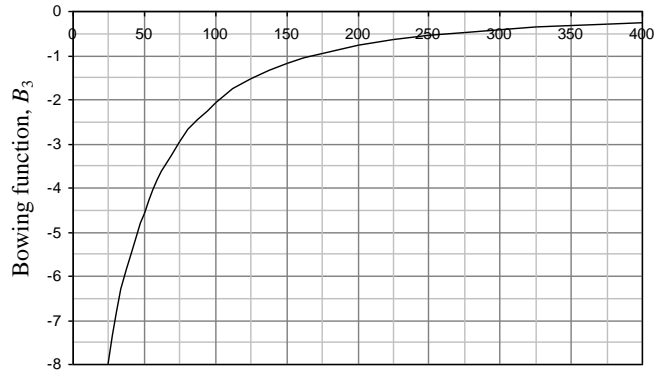


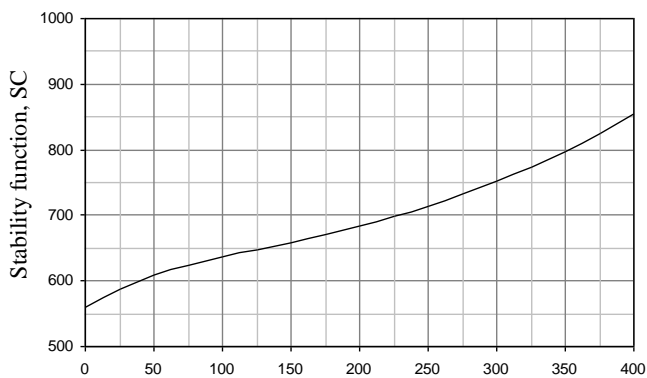
Figure (5) Stability and bowing functions for concave configuration beam-column in tapering ratio $u = 4.0$



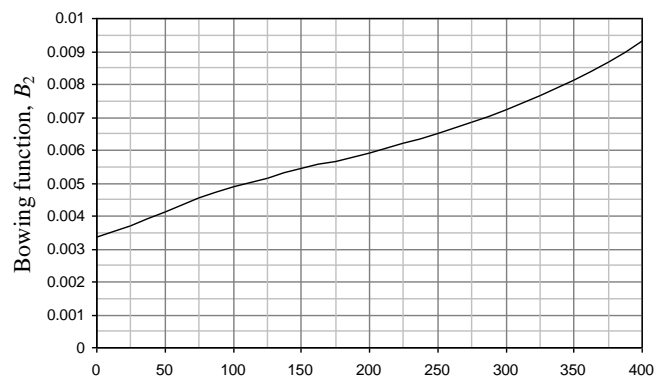
Non-dimensional axial force parameter, ρ_2



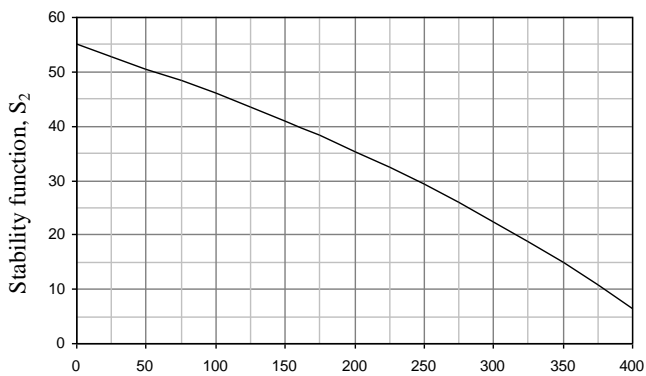
Non-dimensional axial force parameter, ρ_2



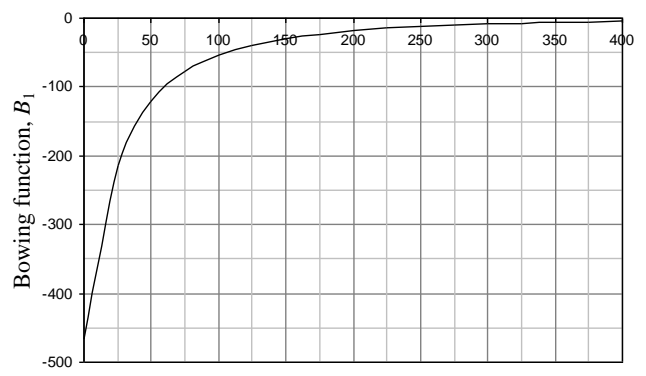
Non-dimensional axial force parameter, ρ_2



Non-dimensional axial force parameter, ρ_2



Non-dimensional axial force parameter, ρ_2



Non-dimensional axial force parameter, ρ_2

Figure (6) Stability and bowing functions for concave configuration beam-column in tapering ratio $u = 5.0$

5. The Finite Element Method

5-1 Stiffness Matrix

For a prismatic beam element, Fig.(7), the displacement field may be assumed as:

$$v(x) = a_1 + a_2x + a_3x^2 + a_4x^3 \dots\dots\dots (48)$$

and in matrix form:

$$v(x) = [x] \{a\} \dots\dots\dots (49)$$

$$v'(x) = \theta(x) = [x'] \{a\} \dots\dots\dots (50)$$

where:

$$[x] = [1 \quad x \quad x^2 \quad x^3]$$

$$[x'] = [0 \quad 1 \quad 2x \quad 3x^2]$$

Hence the nodal displacements {d} will be:

$$\{d\} = \begin{Bmatrix} v_1 \\ \theta_1 \\ v_2 \\ \theta_2 \end{Bmatrix} = \begin{bmatrix} 1 & 0 & 0 & 0 \\ 0 & 1 & 0 & 0 \\ 1 & L & L^2 & L^3 \\ 0 & 1 & 2L & 3L^2 \end{bmatrix} \begin{Bmatrix} a_1 \\ a_2 \\ a_3 \\ a_4 \end{Bmatrix} \dots\dots\dots (51)$$

$$\{d\} = [A] \{a\} \dots\dots\dots (52)$$

$$\{a\} = [A]^{-1} \{d\} \dots\dots\dots (53)$$

By substituting Equation (53) into Equation (49) yields:

$$v(x) = [x] [A]^{-1} \{d\} \dots\dots\dots (54)$$

where:

$$[A]^{-1} = \begin{bmatrix} 1 & 0 & 0 & 0 \\ 0 & 1 & 0 & 0 \\ \frac{-3}{L^2} & \frac{-2}{L} & \frac{3}{L^2} & \frac{-1}{L} \\ \frac{2}{L^3} & \frac{1}{L^2} & \frac{-2}{L^3} & \frac{1}{L^2} \end{bmatrix} \dots\dots\dots (55)$$

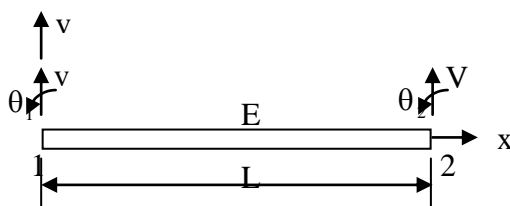


Figure (7) Conventional beam element

For a member subjected to an axial force \$Q\$, the potential energy \$\pi_p\$ is:

$$\pi_p = \frac{EI}{2} \int_0^L \{d\}^T [B]^T [B] \{d\} dx - \frac{Q}{2} \int_0^L \{d\}^T [A]^{-1} [x']^T [x'] [A]^{-1} \{d\} dx \dots\dots\dots (56)$$

where:

$$[K] = \int_0^L [B]^T EI [B] dx \dots\dots\dots (57)$$

$$[k_g] = Q \int_0^L [A]^{-1} [x']^T [x'] [A]^{-1} dx \dots\dots\dots (58)$$

which are the flexural and geometric stiffness matrices respectively for a prismatic element of length \$L\$, hence:

$$[K] = EI \begin{bmatrix} \frac{12}{L^3} & \frac{6}{L^2} & -\frac{12}{L^3} & \frac{6}{L^2} \\ \frac{6}{L^2} & \frac{4}{L} & -\frac{6}{L^2} & \frac{2}{L} \\ -\frac{12}{L^3} & -\frac{6}{L^2} & \frac{12}{L^3} & -\frac{6}{L^2} \\ \frac{6}{L^2} & \frac{2}{L} & -\frac{6}{L^2} & \frac{4}{L} \end{bmatrix} \dots\dots\dots (59)$$

$$[K_g] = Q \begin{bmatrix} \frac{36}{30L} & \frac{1}{10} & -\frac{36}{30L} & \frac{1}{10} \\ \frac{1}{10} & \frac{4L}{30} & -\frac{1}{10} & -\frac{L}{30} \\ \frac{10}{-36} & \frac{30}{-1} & \frac{10}{36} & \frac{30}{-1} \\ \frac{30L}{10} & \frac{10}{-L} & \frac{30L}{10} & \frac{10}{4L} \end{bmatrix} \dots\dots\dots (60)$$

5-2 Solution Procedure

In the present study a beam-column member with a concave configuration is discretized by equivalent prismatic finite elements, **Figure (8)**. The system stiffness matrices $[K]$ and $[K_g]$ are first assembled from the corresponding element matrices. The boundary conditions for the non-prismatic beam-column member then have been applied to the system stiffness matrix $[K-K_g]$. For a specific discretization the buckling load has been obtained by increasing the compressive axial load incrementally until the stiffness $[K-K_g]$ is vanished. The flow chart of the main program is shown in **Fig.(9)**.

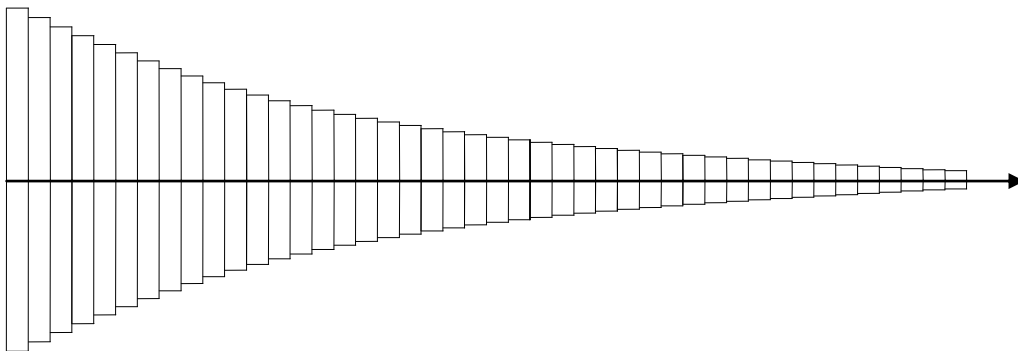


Figure (8) Beam-column-idealization

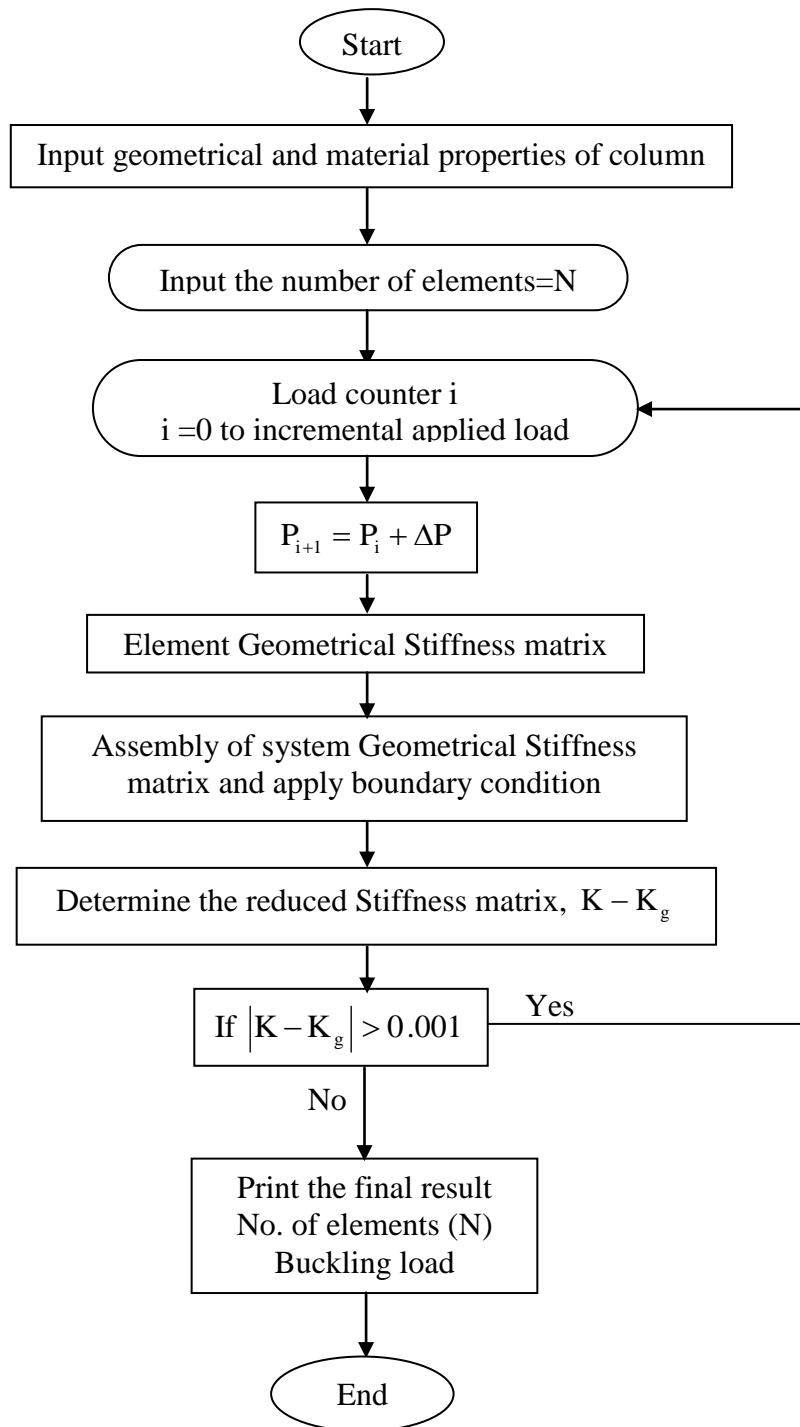


Figure (9) Flow chart of the main finite element program

4. Applications

Application (1):

A beam-column member, which has 5m length, 0.25x0.25 m cross sectional dimensions, $3.2552 \times 10^{-4} \text{ m}^4$ moment of inertia and the modulus of elasticity is 200 GPa, for two models below, in which one end is fixed and the other is hinged and loaded axially as shown in **Fig.(10)**. The elastic critical load for the two models are obtained then compared with others as below:

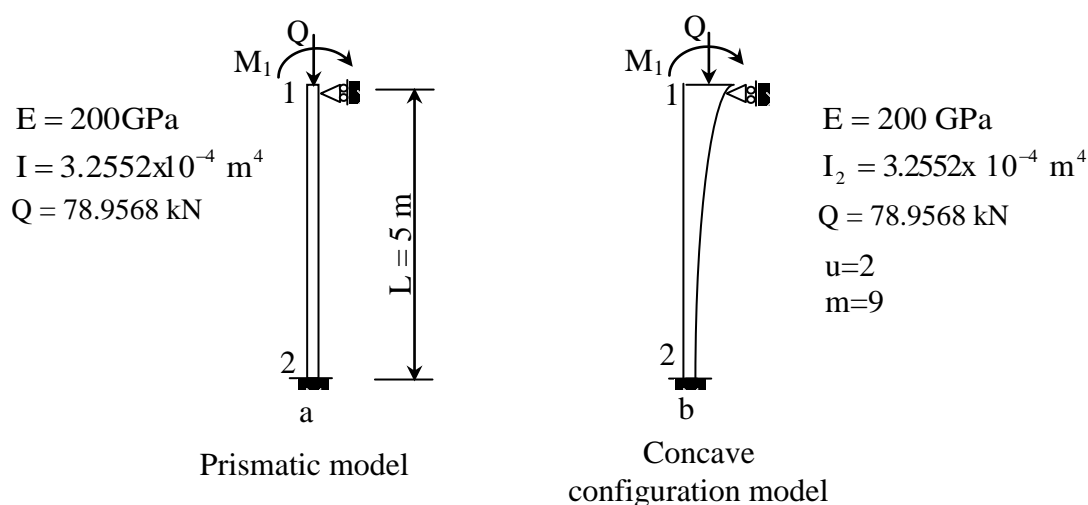


Figure (10) Properties and boundary conditions of the fixed-hinge models

By substituting the boundary condition $\theta_2 = 0$ (at end 2) in the stiffness matrix [T] from Equations (41) the tangent stiffness matrix becomes:

$$[T]\theta_1 = \frac{EI}{L} s\theta_1 \text{ for prismatic member without bowing effect}$$

$$[T]\theta_1 = \frac{EI_2}{L} S_1\theta_1 \text{ for concave configuration member without bowing effect}$$

$$[T]\theta_1 = \frac{EI_2}{L} \left(S_1 + \frac{G_1^2}{\pi^2 H} \right) \theta_1 \text{ for concave configuration member with bowing effect}$$

The non-dimensional axial load parameter which is making the stiffness matrix [T] to vanish is obtained by trial and error with interpolation, using above Equations $s=0$ at $\rho = 2.0457$, $S_1 = 0$ at $\rho = 28.71804$ from **Fig.(3)**, $S_1 + \frac{G_1^2}{\pi^2 H} = 0$ at ρ given in **Appendix-C** for different values of θ_1 .

The above non-prismatic members are solved with different tapering ratio from $u=1$ up to 5, then the elastic critical load of members are drawn for all tapering ratio in **Fig.(11)**.

The concave configuration members are solved by using the finite elements method by dividing these members into 50, 100, 150, 200, 250, 300, and 350 equivalent prismatic elements as shown in **Fig.(12)** under increasing axial load until the stiffness [K-Kg] is vanished.

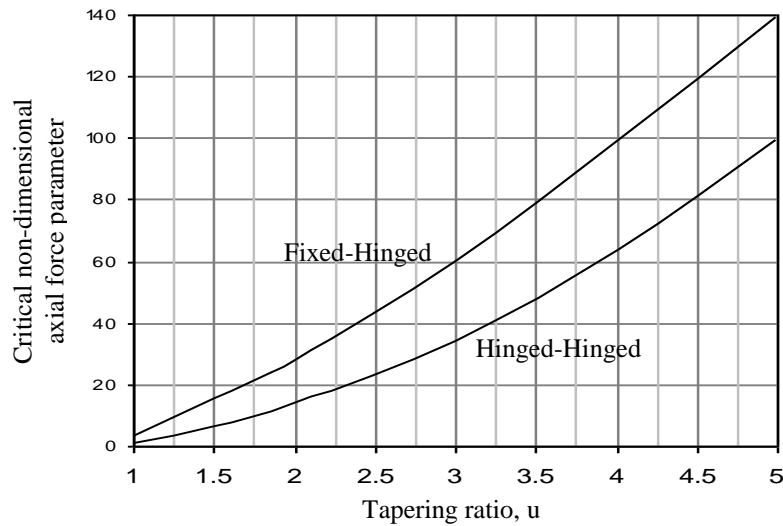


Figure (11) Buckling load of concave members for different tapering ratio

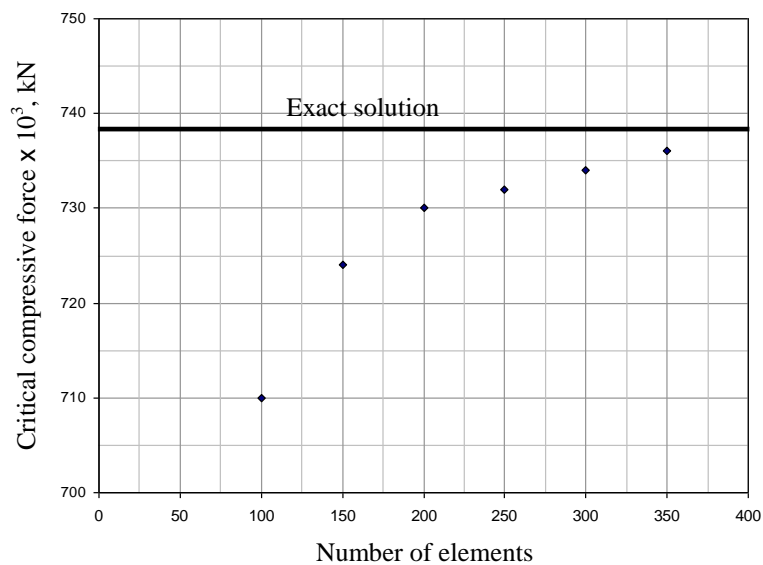


Figure (12) Critical axial force for different number of elements in application 1

Application (2):

A beam-column member, which has the same properties of application (1), but with both ends being hinged. The elastic critical load for the two models are obtained then compared with others as shown in **Fig.(13)** below:

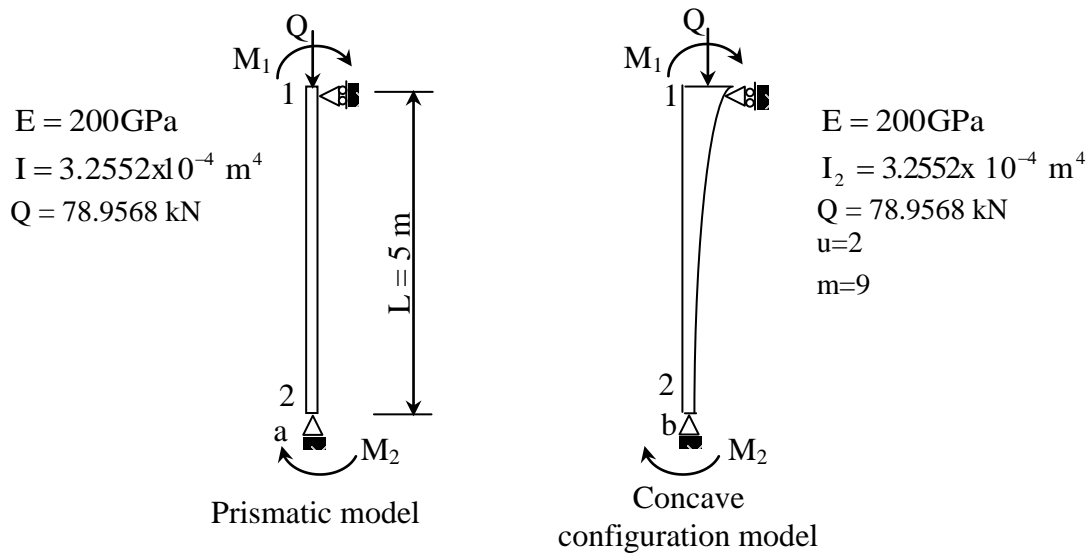


Figure (13) Properties and boundary conditions of the hinge-hinge models

By substituting the boundary condition in the stiffness matrix [T] from Equation (41):

$$[T] \begin{Bmatrix} \theta_1 \\ \theta_2 \end{Bmatrix} = \frac{EI}{L} \begin{bmatrix} s & sc \\ sc & s \end{bmatrix} \begin{Bmatrix} \theta_1 \\ \theta_2 \end{Bmatrix} \quad \text{for prismatic member without bowing effect}$$

$$[T] \begin{Bmatrix} \theta_1 \\ \theta_2 \end{Bmatrix} = \frac{EI_2}{L} \begin{bmatrix} S_1 & SC \\ SC & S_2 \end{bmatrix} \begin{Bmatrix} \theta_1 \\ \theta_2 \end{Bmatrix} \quad \text{for concave configuration member without bowing effect}$$

$$[T] \begin{Bmatrix} \theta_1 \\ \theta_2 \end{Bmatrix} = \frac{EI_2}{L} \begin{bmatrix} \frac{S_1}{u^m} + \frac{G_1^2}{\pi^2 H} & \frac{SC}{u^m} + \frac{G_1 G_2}{\pi^2 H} \\ \frac{SC}{u^m} + \frac{G_1 G_2}{\pi^2 H} & \frac{S_2}{u^m} + \frac{G_2^2}{\pi^2 H} \end{bmatrix} \begin{Bmatrix} \theta_1 \\ \theta_2 \end{Bmatrix} \quad \text{for concave configuration member with bowing effect}$$

The non-dimensional axial load parameter making the stiffness matrix [T] to vanish is obtained by trial and error with interpolation, when $s^2 - sc^2 = 0$ at $\rho = 1$, $S_1 S_2 - SC^2 = 0$ at $\rho = 13.2757$ from **Fig.(3)**, $\left(\frac{S_1}{u^m} + \frac{G_1^2}{\pi^2 H} \right) \left(\frac{S_2}{u^m} + \frac{G_2^2}{\pi^2 H} \right) - \left(\frac{SC}{u^m} + \frac{G_1 G_2}{\pi^2 H} \right)^2 = 0$ at ρ given in appendix-C for different values of θ_1 and θ_2 .

The above non-prismatic members are solved with different tapering ratio from $u=1$ up to 5, then the elastic critical load of members is drawn for all tapering ratio in **Fig.(11)**.

The concave configuration members are solved by using finite elements method by dividing these members into 50, 100, 150, 200, 250, 300, and 350 equivalent prismatic elements as shown in **Fig.(14)** under increasing axial load until the stiffness [K-Kg] is vanished.

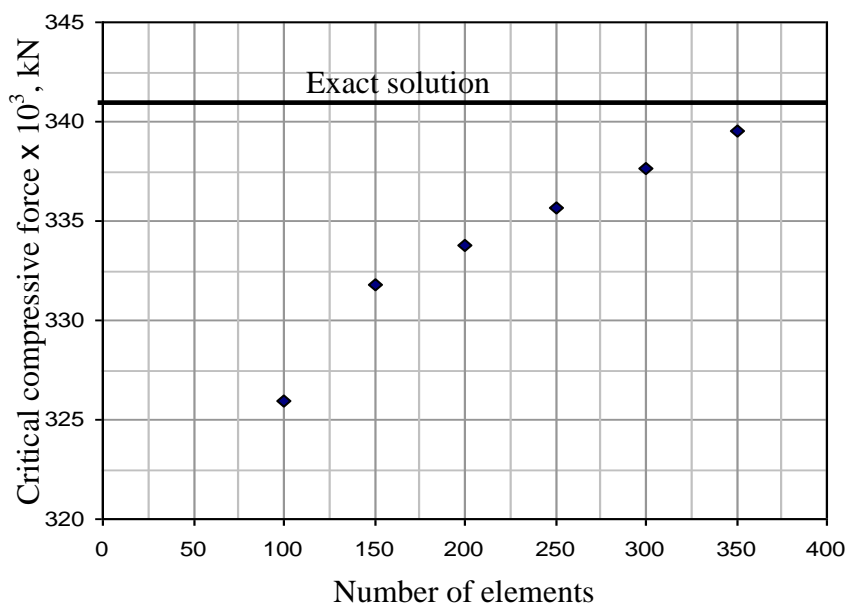


Figure (14) Critical axial force for different number of elements in application 2

5. Conclusion

The pre-buckling forces and deformations are considered until the beam-column buckles under load named the critical axial force. This consideration is done by deriving the stability and bowing functions for concave configuration of beam-column then compared with prismatic one.

The elastic critical load depends on the stiffness of member and support type as explained in the two previous applications, which increased in the concave shape to 1404% and 1328% when compared with the prismatic shape at the supporting type of member fixed-hinged and hinged-hinged respectively. The bowing effects physically represent the apparent shortening and bowing chord of beam-column element that produced an additional stiffness.

In application (1) the elastic critical load of beam-column member increased with the increasing of rotations at the ends of member starting from 100.01387% to 100.1222% when rotations equal to 0.1 and 1.0 radian respectively, when compared with the elastic critical load without bowing effect.

In application (2) the elastic critical load of beam-column member increased with the increasing of rotations at the ends of member starting from 100.01067% to 100.1222% when rotations equal to 0.1 and 1.0 radian respectively, when compared with the elastic critical load without bowing effect.

These functions of stability and bowing are presented graphically in five different tapering ratios with respect to the non-dimensional axial force parameter for beam-column subjected to compressive axial force.

6. References

- 1. Yossif, W. V., “*Modified Stability Functions with Shear Effect for Non-Prismatic Members in Steel Plane Frames and Member Inside Soils*”, Ph.D. Thesis, University of Baghdad, Baghdad April 2006.**
- 2. Goto Y., Suzuki, S., and Chen, W., “*Bowing Effect on Elastic Stability of Frames under Primary Bending Moments*”, Journal of Structural Division, ASCE, Vol. 117, No. 1, January 1991.**
- 3. Oran, C., “*Tangent Stiffness in Plane Frames*”, Journal of Structural Division, ASCE, Vol. 99, No. ST6, June 1973, pp. 973-985.**
- 4. Oran, C., “*Tangent Stiffness in Space Frames*”, Journal of Structural Division, ASCE, Vol. 100, No. ST7, July 1973, pp. 987-1001.**
- 5. McLachlan, N. W., “*Bessel Functions for Engineering*”, Clarendon Press Oxford, 1961.**
- 6. Al-Sarraf, S. Z., “*Elastic Instability of Frames with Uniformly Tapered Members*”, The Structural Engineer, March 1979, 18pp.**
- 7. Al-Sarraf, S. Z., and Yossif, W. V., “*Elastic Instability of Frames with Non-linear Tapered Members*”, Journal of Babylon University, Vol. 13, No. 5, 2005.**
- 8. Chan, S., and Gu, J., “*Exact Tangent Stiffness for Imperfect Beam-Column Members*”, Journal of Structural Division, ASCE, Vol. 126, No. 9, September 2000, pp. 1094.**

Appendix A

Symbol	Equations
g_1	$\left(h_1 - h_4 - \frac{Z'}{\omega}\right)\left(\frac{1}{\rho} + \frac{Z'}{Z} + \frac{\omega'}{\omega} - \frac{P'}{P}\right)$
g_2	$\left(h_2 - h_5 - \frac{Z'}{\omega}\right)\left(\frac{1}{\rho} + \frac{Z'}{Z} + \frac{\omega'}{\omega} - \frac{P'}{P}\right)$
g_3	$\left(-h_3 + h_6 + \frac{Z'}{\omega}\right)\left(\frac{1}{\rho} + \frac{Z'}{Z} + \frac{\omega'}{\omega} - \frac{P'}{P}\right)$
g_4	$h'_1 - h'_4 - \left(\frac{Z''}{Z'} - \frac{\omega'}{\omega}\right)\left(\frac{Z'}{\omega}\right)$
g_5	$h'_2 - h'_5 - \left(\frac{Z''}{Z'} - \frac{\omega'}{\omega}\right)\left(\frac{Z'}{\omega}\right)$
g_6	$-h'_3 + h'_6 + \left(\frac{Z''}{Z'} - \frac{\omega'}{\omega}\right)\left(\frac{Z'}{\omega}\right)$

Symbol	Equations
h_1	$\left(\frac{f_4 L}{a^{1.2}} + \frac{Z}{\omega}\right)\left(\frac{P'}{P} - \frac{Z'}{Z} - \frac{1}{\rho}\right)$
h_2	$\left(\frac{f_3 L}{b^{1.2}} + \frac{Z}{\omega}\right)\left(\frac{P'}{P} - \frac{Z'}{Z} - \frac{1}{\rho}\right)$
h_3	$\left(\frac{f_6 L}{a^{0.7} b^{0.5}} + \frac{Z}{\omega}\right)\left(\frac{P'}{P} - \frac{Z'}{Z} - \frac{1}{\rho}\right)$
h_4	$\frac{f_4 L}{a^{1.2}}\left(\frac{\omega'}{\omega} + \frac{f'_4}{f_4}\right)$
h_5	$\frac{f_3 L}{b^{1.2}}\left(\frac{\omega'}{\omega} + \frac{f'_3}{f_3}\right)$
h_6	$\frac{f_6 L}{a^{0.7} b^{0.5}}\left(\frac{\omega'}{\omega} + \frac{f'_6}{f_6}\right)$

Symbol	Equations
f_1	$J_{-1.143}(\alpha)J_{1.143}(\beta) - J_{1.143}(\alpha)J_{-1.143}(\beta)$
f_2	$J_{-0.143}(\alpha)J_{0.143}(\beta) - J_{0.143}(\alpha)J_{-0.143}(\beta)$
f_3	$J_{0.143}(\alpha)J_{1.143}(\beta) + J_{0.143}(\alpha)J_{-1.143}(\beta)$
f_4	$J_{-0.143}(\beta)J_{1.143}(\alpha) + J_{0.143}(\beta)J_{-1.143}(\alpha)$
f_5	$J_{0.143}(\beta)J_{-1.143}(\beta) + J_{-0.143}(\beta)J_{1.143}(\beta)$
f_6	$J_{-0.143}(\alpha)J_{1.143}(\alpha) + J_{0.143}(\alpha)J_{-1.143}(\alpha)$

Symbol	Equations
h'_1	$\left(\frac{P'}{P} - \frac{Z'}{Z} - \frac{1}{\rho}\right)h'_{1a} + \left(\frac{f_4 L}{a^{4.5}} + \frac{Z}{\omega}\right)h'_{1b}$
h'_2	$\left(\frac{P'}{P} - \frac{Z'}{Z} - \frac{1}{\rho}\right)h'_{1a} + \left(\frac{f_3 L}{b^{4.5}} + \frac{Z}{\omega}\right)h'_{1b}$
h'_3	$\left(\frac{P'}{P} - \frac{Z'}{Z} - \frac{1}{\rho}\right)h'_{1a} + \left(\frac{f_6 L}{a^4 b^{0.5}} + \frac{Z}{\omega}\right)h'_{1b}$
h'_4	$\frac{f_4 \omega' L}{\omega a^{4.5}}\left(\frac{\omega''}{\omega'} - \frac{\omega'}{\omega} + \frac{f'_4}{f_4}\right) + \frac{f_4'' L}{a^{4.5}}$
h'_5	$\frac{f_3 \omega' L}{\omega b^{4.5}}\left(\frac{\omega''}{\omega'} - \frac{\omega'}{\omega} + \frac{f'_3}{f_3}\right) + \frac{f_3'' L}{b^{4.5}}$
h'_6	$\frac{f_6 \omega' L}{\omega a^4 b^{0.5}}\left(\frac{\omega''}{\omega'} - \frac{\omega'}{\omega} + \frac{f'_6}{f_6}\right) + \frac{f_6'' L}{a^4 b^{0.5}}$

Symbol	Equations
h'_{1a}	$\frac{f'_4 L}{a^{4.5}} + \frac{Z'}{\omega} - \frac{\omega' Z}{\omega^2}$
h'_{2a}	$\frac{f'_3 L}{b^{4.5}} + \frac{Z'}{\omega} - \frac{\omega' Z}{\omega^2}$
h'_{3a}	$\frac{f'_6 L}{a^4 b^{0.5}} + \frac{Z'}{\omega} - \frac{\omega' Z}{\omega^2}$

Symbol	Equations
h'_{1b}	$\frac{P''}{P} - \frac{Z''}{Z} + \frac{1}{\rho^2} - \left(\frac{P'}{P}\right)^2 + \left(\frac{Z'}{Z}\right)^2$
h'_{2b}	$\frac{P''}{P} - \frac{Z''}{Z} + \frac{1}{\rho^2} - \left(\frac{P'}{P}\right)^2 + \left(\frac{Z'}{Z}\right)^2$
h'_{3b}	$\frac{P''}{P} - \frac{Z''}{Z} + \frac{1}{\rho^2} - \left(\frac{P'}{P}\right)^2 + \left(\frac{Z'}{Z}\right)^2$

Symbol	Equations
$J'_{0.143}(\alpha)$	$\left(\frac{0.143}{\alpha} J_{0.143}(\alpha) - J_{1.143}(\alpha)\right)\alpha'$
$J'_{-0.143}(\alpha)$	$\left(\frac{-0.143}{\alpha} J_{-0.143}(\alpha) - J_{-1.143}(\alpha)\right)\alpha'$
$J'_{0.143}(\beta)$	$\left(\frac{0.143}{\beta} J_{0.143}(\beta) - J_{1.143}(\beta)\right)\beta'$
$J'_{-0.143}(\beta)$	$\left(\frac{-0.143}{\beta} J_{-0.143}(\beta) - J_{-1.143}(\beta)\right)\beta'$

Symbol	Equations
$J'_{1.143}(\alpha)$	$\left(\frac{1.143}{\alpha} J_{1.143}(\alpha) + J_{0.143}(\alpha)\right)\alpha'$
$J'_{-1.143}(\alpha)$	$\left(\frac{-1.143}{\alpha} J_{-1.143}(\alpha) + J_{-0.143}(\alpha)\right)\alpha'$
$J'_{1.143}(\beta)$	$\left(\frac{1.143}{\beta} J_{1.143}(\beta) + J_{0.143}(\beta)\right)\beta'$
$J'_{-1.143}(\beta)$	$\left(\frac{-1.143}{\beta} J_{-1.143}(\beta) + J_{-0.143}(\beta)\right)\beta'$

Symbol	Equations
f'_1	$J'_{-1.143}(\alpha)J_{1.143}(\beta) + J'_{1.143}(\beta)J_{-1.143}(\alpha) - f_{11}$
f'_2	$J_{0.143}(\beta)J'_{-0.143}(\alpha) + J'_{0.143}(\beta)J_{-0.143}(\alpha) - f_{22}$
f'_3	$J_{-0.143}(\alpha)J'_{1.143}(\beta) + J'_{-0.143}(\alpha)J_{1.143}(\beta) + f_{33}$
f'_4	$J_{-0.143}(\beta)J'_{1.143}(\alpha) + J'_{-0.143}(\beta)J_{1.143}(\alpha) + f_{44}$
f'_5	$J_{0.143}(\beta)J'_{-1.143}(\beta) + J'_{0.143}(\beta)J_{-1.143}(\beta) + f_{55}$
f'_6	$J_{-0.143}(\alpha)J'_{1.143}(\alpha) + J'_{-0.143}(\alpha)J_{1.143}(\alpha) + f_{66}$

Symbol	Equations
f_{11}	$J'_{1.143}(\alpha)J_{-1.143}(\beta) + J_{1.143}(\alpha)J'_{-1.143}(\beta)$
f_{22}	$J'_{0.143}(\alpha)J_{-0.143}(\beta) + J'_{-0.143}(\beta)J_{0.143}(\alpha)$
f_{33}	$J_{0.143}(\alpha)J'_{-1.143}(\beta) + J'_{0.143}(\alpha)J_{-1.143}(\beta)$
f_{44}	$J_{0.143}(\beta)J'_{-1.143}(\alpha) + J'_{0.143}(\beta)J_{-1.143}(\alpha)$
f_{55}	$J_{-0.143}(\beta)J'_{1.143}(\beta) + J'_{-0.143}(\beta)J_{1.143}(\beta)$
f_{66}	$J_{0.143}(\alpha)J'_{-1.143}(\alpha) + J'_{0.143}(\alpha)J_{-1.143}(\alpha)$

Symbol	Equations
$J''_{0.143}(\alpha)$	$\left[\frac{-0.143\alpha'}{\alpha^2} J_{0.143}(\alpha) + \frac{0.143}{\alpha} J'_{0.143}(\alpha) - J'_{1.143}(\alpha)\right]\alpha' + \left(\frac{0.143}{\alpha} J_{0.143}(\alpha) - J_{1.143}(\alpha)\right)\alpha''$
$J''_{-0.143}(\alpha)$	$\left[\frac{-0.143\alpha'}{\alpha^2} J_{-0.143}(\alpha) + \frac{0.143}{\alpha} J'_{-0.143}(\alpha) + J'_{-1.143}(\alpha)\right]\alpha' + \left(\frac{0.143}{\alpha} J_{-0.143}(\alpha) + J_{-1.143}(\alpha)\right)\alpha''$
$J''_{0.143}(\beta)$	$\left[\frac{-0.143\beta'}{\beta^2} J_{0.143}(\beta) + \frac{0.143}{\beta} J'_{0.143}(\beta) - J'_{1.143}(\beta)\right]\beta' + \left(\frac{0.143}{\beta} J_{0.143}(\beta) - J_{1.143}(\beta)\right)\beta''$
$J''_{-0.143}(\beta)$	$\left[\frac{-0.143\beta'}{\beta^2} J_{-0.143}(\beta) + \frac{0.143}{\beta} J'_{-0.143}(\beta) + J'_{-1.143}(\beta)\right]\beta' + \left(\frac{0.143}{\beta} J_{-0.143}(\beta) + J_{-1.143}(\beta)\right)\beta''$
$J''_{1.143}(\alpha)$	$\left[\frac{1.143\alpha'}{\alpha^2} J_{1.143}(\alpha) - \frac{1.143}{\alpha} J'_{1.143}(\alpha) + J'_{0.143}(\alpha)\right]\alpha' + \left(\frac{-1.143}{\alpha} J_{1.143}(\alpha) + J_{0.143}(\alpha)\right)\alpha''$
$J''_{-1.143}(\alpha)$	$\left[\frac{1.143\alpha'}{\alpha^2} J_{-1.143}(\alpha) - \frac{1.143}{\alpha} J'_{-1.143}(\alpha) - J'_{-0.143}(\alpha)\right]\alpha' + \left(\frac{-1.143}{\alpha} J_{-1.143}(\alpha) - J_{-0.143}(\alpha)\right)\alpha''$
$J''_{1.143}(\beta)$	$\left[\frac{1.143\beta'}{\beta^2} J_{1.143}(\beta) - \frac{1.143}{\beta} J'_{1.143}(\beta) + J'_{0.143}(\beta)\right]\beta' + \left(\frac{-1.143}{\beta} J_{1.143}(\beta) + J_{0.143}(\beta)\right)\beta''$
$J''_{-1.143}(\beta)$	$\left[\frac{1.143\beta'}{\beta^2} J_{-1.143}(\beta) - \frac{1.143}{\beta} J'_{-1.143}(\beta) - J'_{-0.143}(\beta)\right]\beta' + \left(\frac{-1.143}{\beta} J_{-1.143}(\beta) - J_{-0.143}(\beta)\right)\beta''$

Symbol	Equations
f_1''	$2J'_{1.143}(\beta)J'_{-1.143}(\alpha) + J''_{1.143}(\beta)J_{-1.143}(\alpha) - 2J'_{-1.143}(\beta)J'_{1.143}(\alpha) - J''_{-1.143}(\beta)J_{1.143}(\alpha) + J_{1.143}(\beta)J''_{-1.143}(\alpha) - J_{-1.143}(\beta)J''_{1.143}(\alpha)$
f_2''	$2J'_{0.143}(\beta)J'_{-0.143}(\alpha) + J''_{0.143}(\beta)J_{-0.143}(\alpha) - 2J'_{-0.143}(\beta)J'_{0.143}(\alpha) - J''_{-0.143}(\beta)J_{0.143}(\alpha) + J_{0.143}(\beta)J''_{-0.143}(\alpha) - J_{-0.143}(\beta)J''_{0.143}(\alpha)$
f_3''	$2J'_{-0.143}(\alpha)J'_{1.143}(\beta) + J''_{-0.143}(\alpha)J_{1.143}(\beta) + 2J'_{0.143}(\alpha)J'_{-1.143}(\beta) + J''_{0.143}(\alpha)J_{-1.143}(\beta) + J_{-0.143}(\alpha)J''_{1.143}(\beta) + J_{0.143}(\alpha)J''_{-1.143}(\beta)$
f_4''	$2J'_{-0.143}(\beta)J'_{1.143}(\alpha) + J''_{-0.143}(\beta)J_{1.143}(\alpha) + 2J'_{0.143}(\beta)J'_{-1.143}(\alpha) + J''_{0.143}(\beta)J_{-1.143}(\alpha) + J_{-0.143}(\beta)J''_{1.143}(\alpha) + J_{0.143}(\beta)J''_{-1.143}(\alpha)$
f_5''	$2J'_{0.143}(\beta)J'_{-1.143}(\alpha) + J''_{0.143}(\beta)J_{-1.143}(\alpha) + 2J'_{-0.143}(\beta)J'_{1.143}(\alpha) + J''_{-0.143}(\beta)J_{1.143}(\alpha) + J_{0.143}(\beta)J''_{-1.143}(\alpha) + J_{-0.143}(\beta)J''_{1.143}(\alpha)$
f_6''	$2J'_{-0.143}(\alpha)J'_{1.143}(\beta) + J''_{-0.143}(\alpha)J_{1.143}(\beta) + 2J'_{0.143}(\alpha)J'_{-1.143}(\beta) + J''_{0.143}(\alpha)J_{-1.143}(\beta) + J_{-0.143}(\alpha)J''_{1.143}(\beta) + J_{0.143}(\alpha)J''_{-1.143}(\beta)$

Symbol	Equations	Symbol	Equations
P_1	$Z\omega \left[a^4 \left(\frac{f'_3}{a^{-0.5}} - \frac{f'_5}{b^{-0.5}} \right) + b^4 \left(\frac{f'_4}{b^{-0.5}} - \frac{f'_6}{a^{-0.5}} \right) \right]$	Z	$J_{0.143}(\alpha)J_{-0.143}(\beta) - J_{-0.143}(\alpha)J_{0.143}(\beta)$
P_2	$\left(\frac{\omega'}{\omega} + \frac{Z'}{Z} - \frac{P_1}{P'} \right) \frac{P'}{P} + \frac{\omega''}{\omega} + \frac{Z''}{Z} - \left(\frac{\omega'}{\omega} \right)^2$	Z'	$Z_1 + Z_2$
P_3	$\left(\frac{f'_2}{f_2} + \frac{f'_1}{f_1} + \frac{\omega'}{\omega} \right) \frac{\omega'}{\omega} + \frac{f'_1}{f_1} \left(\frac{f'_2}{f_2} + 2 \frac{\omega'}{\omega} \right)$	Z''	$Z'_1 + Z'_2 + Z'_3$
P_4	$a^4 \left(\frac{f''_3}{a^{-0.5}} - \frac{f''_5}{b^{-0.5}} \right) + b^4 \left(\frac{f''_4}{b^{-0.5}} - \frac{f''_6}{a^{-0.5}} \right)$	Z_1	$J'_{0.143}(\alpha)J_{-0.143}(\beta) - J'_{-0.143}(\alpha)J_{0.143}(\beta)$
P_5	$Z\omega \left[a^4 \left(\frac{f_3}{a^{-0.5}} - \frac{f_5}{b^{-0.5}} \right) + b^4 \left(\frac{f_4}{b^{-0.5}} - \frac{f_6}{a^{-0.5}} \right) \right]$	Z_2	$J_{0.143}(\alpha)J'_{-0.143}(\beta) - J_{-0.143}(\alpha)J'_{0.143}(\beta)$
P'_1	$Z\omega \left[\left(\frac{Z'}{Z} + \frac{\omega'}{\omega} \right) \left(\frac{P_1}{\omega Z} \right) + P_4 \right]$	Z'_1	$2J'_{-0.143}(\beta)J'_{0.143}(\alpha) - 2J'_{-0.143}(\alpha)J'_{0.143}(\beta)$
P	$-\left(\omega^2 L f_1 f_2 + P_5 \right)$	Z'_2	$J''_{-0.143}(\beta)J_{0.143}(\alpha) - J_{-0.143}(\alpha)J''_{0.143}(\beta)$
P'	$\left[\left(\frac{\omega'}{\omega} + \frac{Z'}{Z} \right) P - \left(\frac{\omega'}{\omega} + \frac{f'_1}{f_1} \right) \omega^2 L f_1 f_2 \right] - P_1$	Z'_3	$J''_{0.143}(\alpha)J_{-0.143}(\beta) - J''_{-0.143}(\alpha)J_{0.143}(\beta)$
P''	$\left[P_2 - \left(\frac{Z'}{Z} \right)^2 \right] P - \left(P_3 + \frac{f''_1}{f_1} + \frac{\omega''}{\omega} \right) \omega^2 L f_1 f_2$		

Appendix B

$$\frac{\partial \rho_2}{\partial \theta_1} = \frac{G_1}{\pi^2 H}, \quad \frac{\partial \rho_2}{\partial \theta_2} = \frac{G_2}{\pi^2 H}, \quad \frac{\partial \rho_2}{\partial (U/L)} = \frac{\lambda^2}{\pi^2}$$

$$\frac{\partial M_1}{\partial \rho_2} = \frac{EI_2}{L} G_1, \quad \frac{\partial M_2}{\partial \rho_2} = \frac{EI_2}{L} G_2, \quad \frac{\partial (QL)}{\partial \rho_2} = \frac{EI_2}{L} \lambda^2 H$$

$$\frac{\partial M_1}{\partial \theta_1} = \frac{EI_2}{Lu^m} S_1, \quad \frac{\partial M_1}{\partial \theta_2} = \frac{\partial M_2}{\partial \theta_1} = \frac{EI_2}{Lu^m} SC, \quad \frac{\partial M_2}{\partial \theta_2} = \frac{EI_2}{Lu^m} S_2$$

Appendix C

Application (1)

θ_1	0.1	0.2	0.4	1.0
θ_2	0.0	0.0	0.0	0.0
β_1	0.036214	0.036214	0.036214	0.036214
β_3	-0.078591	-0.078591	-0.078591	-0.078591
β'_1	0.785629	0.785629	0.785629	0.785629
A_0	0.09017	0.09017	0.09017	0.09017
λ	83.217	83.217	83.217	83.217
G_1	-0.07148	-0.143	-0.286	-0.7148
G_2	0.15513	0.31026	0.62052	1.5513
H	0.0092815	0.03285	0.12713	0.78705
$G_1^2 / \pi^2 H$	0.0558	0.06307	0.0652	0.5109
S_1	-0.0558	-0.06307	-0.0652	-0.5109
ρ_2	28.722023	28.722522	28.72267	28.75316
%	100.01387	100.01561	100.01612	100.1222
Difference	0.003983	0.004482	0.00463	0.03512

Application (2)

θ_1	0.1	0.2	0.4	1
θ_2	0.1	0.2	0.4	1
β_1	0.02209	0.02209	0.02209	0.02209
β_2	0.459	0.459	0.459	0.459
β_3	-0.031589	-0.031589	-0.031589	-0.031589
β'_1	3.91772	3.91772	3.91772	3.91772
β'_2	7.242	7.242	7.242	7.242
β'_3	14.461	14.461	14.461	14.461
A_0	0.09017	0.09017	0.09017	0.09017
λ	83.217	83.217	83.217	83.217
G_1	-0.94963	-1.89926	-3.79853	-9.49633
G_2	-0.84368	-1.68735	-3.37470	-8.43675
H	0.3300	1.31593	5.2594	10.8575
$G_1^2 / \pi^2 H$	0.27688	0.27774	0.27796	0.84155
$G_2^2 / \pi^2 H$	0.21854	0.21922	0.21940	0.66424
$G_1 G_2 / \pi^2 H$	0.246	0.2465	0.247	0.74766
S_1	175.533	175.5325	175.532	175.5304
S_2	10.009	10.009	10.009	10.0088
SC	41.915	41.915	41.915	41.916
ρ_2	13.27713	13.27718	13.27725	13.29222
%	100.01067	100.01101	100.01172	100.1222
Diff.	0.001444	0.001494	0.001564	0.016534

Notice: The percent is the ratio of the non-dimensional axial force parameter including to the excluding bowing effects and the diff is the difference between the value of the non-dimensional axial force parameter including and excluding bowing effects.